JOURNAL OF MATERIALS SCIENCE 28 (1993) 3353–3366

Study of carbon fibre surface treatments by dynamic mechanical analysis

B. HARRIS, O. G. BRADDELL*, D. P. ALMOND
School of Materials Science, University of Bath, Bath BA2 7AY, Avon, UK
C. LEFEBVRE, J. VERBIST
Laboratoire Interdisciplinaire de Spectroscopie Electronique, Facultés Notre-Dame de la Paix, Namur, Belgium

Dynamic mechanical and thermal analysis (DMTA) has been used to study the effects of surface treatment of carbon fibres on the viscoelastic properties of composites containing them. The fibres were treated by dip-coating, electro-polymerization, and plasma polymerization, and the behaviour of these fibres is compared with that of fibres treated by ordinary commercial oxidation and sizing procedures. Analysis of the experimental results is made both in terms of conventional approaches to viscoelastic behaviour and of the power-law analysis of the glass transition in an attempt to obtain suitable parameters for the evaluation of the effects of surface treatment.

1. Introduction

In an earlier paper [1] we presented the results of a EURAM research programme on the surface treatment of carbon fibres by electro-polymerization and plasma polymerization processes. In that paper, it was shown that these methods could be used satisfactorily to graft nitrogen-containing groups, probably amines, on to fibre surfaces and thereby increase the level of bonding between the fibres and the matrix. The techniques used to evaluate the surface treatments were single-fibre tensile testing, resin-impregnated tow testing, and single-fibre composite fragmentation experiments. An additional method of analysis used was that of dynamical mechanical and thermal analysis, or DMTA, and it is the results of this part of the work that form the basis of this second paper.

2. Dynamic mechanical analysis and the study of composites

Dynamic mechanical and thermal analysis has become a widely used technique for the characterization and investigation of polymeric materials. Analysis is based on the determination of the temperature dependences of the dynamic moduli and internal friction, measurements being made whilst the sample is vibrated at a particular frequency, usually in the range 0.1–100 Hz. It has been found that many polymers exhibit characteristic modulus changes and absorption peaks at specific temperatures which are employed as a means of "finger-printing" polymer types and for identifying important properties, such as the glass transition and other transitions.

The dynamic mechanical effects observed in polymers are similar to the phenomena, found in many other materials, that are described as anelastic. The response of an anelastic material to a mechanical stress is not instantaneous but develops by relaxation processes that are characterized by a relaxation time, τ. When the applied stress is periodic, as in a DMTA system, the elastic properties become a function of, $\omega\tau$, the ratio of the angular frequency of the applied stress cycle to the relaxation rate of the material. When $\omega\tau$ is much less than unity, the frequency of the applied stress cycle is low by comparison with the material relaxation rate, $(\tau)^{-1}$, and its elastic response is able to remain in phase with the stress throughout the applied cycle. By contrast, when $\omega\tau$ is much greater than unity the applied frequency is much greater than the natural relaxation rate and the anelastic component of strain is unable to respond to the rapidly changing applied stress. Consequently, as $\omega\tau$ is raised the material appears to stiffen. The analysis has much in common with the classical Debye theory of dielectrics and there is often a close, if not one to one, relationship between mechanical and dielectric relaxation phenomena. Both effects in polymers have been discussed at length in the seminal text by McCrum *et al.* [2].

In addition to changes in elastic moduli, anelasticity leads to the occurrence of mechanical absorption peaks. These are usually presented as peaks in tan δ which is the ratio of the imaginary and real components (otherwise referred to as the loss and storage

* *Present address*: Materials Department, University of Limerick, Plassey Technology Park, Castletroy, Limerick, Ireland.

0022–2461

moduli), M'' and M', respectively, of the complex elastic modulus, given by $M^* = M' - iM''$. An expression for tan δ is [1]

$$\tan\delta = B\frac{\omega\tau}{[1 + \omega^2(\tau_{eff})^2]} \quad (1)$$

where $B = (M_U - M_R)/(M_U M_R)^{1/2}$, M_R and M_U being, respectively, the relaxed and unrelaxed moduli of the material, and τ_{eff} is an effective relaxation time, $\tau_{eff} = (\tau_\sigma \tau_\varepsilon)^{1/2}$, where τ_σ and τ_ε are the true relaxation times associated with a constant stress or constant strain experiment. The function for tan δ reaches a maximum when $\omega\tau_{eff} = 1$. The relaxation time often falls with temperature in the thermally activated Arrhenius fashion

$$\tau_{eff} = \tau_o \exp(E_a/kT) \quad (2)$$

in which E_a is an activation energy, τ_o^{-1} is an attempt frequency and k is the Boltzmann constant. Thus a mechanical absorption peak may be generated by sweeping a temperature range, the peak occurring at the temperature for which the relaxation time satisfies the condition $\omega\tau_{eff} = 1$.

Changes in viscoelastic characteristics are also sometimes illustrated by the Cole–Cole method, originally developed for the study of dielectric dispersion [3], of representing the complex modulus, M^*, as the relationship between M'' and M' in the complex plane. For the ideal Debye solid of Equation 1, this relationship is encompassed in the equation

$$(M^* - M_R) = (M_U - M_R)/(1 + i\omega\tau_{eff}) \quad (3)$$

and an M'' versus M' plot gives a semi-circle of diameter $(M_U - M_R)$, with its centre on the M' axis, which is the locus of the complex modulus as ω varies from 0 to ∞.

The DMTA method is thus a sensitive means of detecting changes in the mobility of molecules and for investigating phase structure and morphology. For polymeric materials, it is able to identify a range of relaxations and transitions, and is thus a potentially powerful tool for assessing the effects of such features of composite materials as matrix polymer modification (e.g. "flexiblization"), matrix crystallinity, transcrystallinity at a fibre/thermoplastic matrix interface, and interphase behaviour or other effects of fibre-surface treatments [4–16].

2.1. Some results of DMTA studies of the interface/interphase

The region in a composite at the interface between a rigid carbon or glass fibre and a cured thermoset resin is likely to consist of a chemically and physically complex polymer species with characteristics different from those of the normal bulk matrix, even without the interpolation of the sizes or coupling agents that are applied as a matter of course to commercial reinforcing fibres. In the brief survey which follows, therefore, we shall refer to studies that bear upon this aspect of composite behaviour in addition to those which deal specifically with deliberately interposed fibre coatings, because the effects of the two types of interphase may not easily be distinguishable. A number of workers have claimed that it is possible by means of DMTA experiments to detect the effects of interphases or fibre surface treatments, particularly through their influence on the characteristics of the loss peaks. An early DMTA study of the interphase which results from polymer/filler interaction, that of Theocaris and Papanicolaou [4], suggested that the temperature of the α peak of an epoxy resin was significantly higher (25 K) in the bulk resin than in glass-fibre composites containing the same resin, and that the T_g value for the composite was reduced by about 20 K as the orientation of the fibres relative to the sample axis shifted from 0° to 90°. They developed a geometric, concentric cylinder model which accurately explains the latter effect, but they offer no clear explanation of the former beyond observing that the characteristics of the resin are likely to be influenced by the presence of the rigid fibre surface and the fibre size.

Chua [14] studied the effects of organo-silane coatings on glass fibres and found that there was an inverse linear correlation between the height of the tan δ peak at T_g and the interfacial shear strength of glass/polyester composites as determined by the quantity of organo-silane on the fibre surface. An increase in the thickness of the coating led to an increase in the peak height. He also reported [15] that the tan δ peak height, measured in both the axial and transverse orientations relative to the fibres, varied inversely with both the interlaminar shear strength (ILSS) and the transverse flexural strength, suggesting a direct correlation between the mechanical loss, or internal friction, and the ILSS. He suggested that an organo-silane coating with unreactive organic groups leads to an interphase with many unrestrained or free end groups which results in a reduction in the cross-link density of the polymer network in the interphase region. This plasticized region then gives increased internal friction, but reduces the interfacial bond strength (as characterized by the ILSS).

Chabert and co-workers [9–11, 16] have published widely on this subject and have used dynamic mechanical analysis to study the effects of coatings on both glass and carbon fibres. For unidirectional glass/epoxy composites, for example, they showed [9] that whereas the temperature of the glass transition was largely unaffected by introducing fibres with different types of sizing and it was not possible to distinguish between two size coatings of quite different character by the peak height, the presence of an amino-silane coupling agent resulted in measurable increases in the relaxation time and the activation energy of the T_g peak. By contrast with the conclusion of Chua, these changes are ascribed to an increase in the rigidity of the interfacial zone resulting from the formation of covalent bonds both between the constituents of the coupling agent itself and between the coupling agent and the glass surface.

In work on carbon-fibre/epoxy composites [10], authors from the same group have given evidence of the effects of surface treatments on both the α and β

peaks. They suggest that the introduction of untreated carbon fibres results in a less cross-linked and more homogeneous structure, with a reduction in the peak height at 0.01 Hz and a broadening of the peak at mid-height. This is in direct contrast to the work of Garton *et al.* [17], for example, who believe that the kinetics of cross-linking is not influenced by the presence of a carbon surface. They also noted that oxidation of the fibre surface to increase the carboxy, carbonyl and phenoxy functionalities has no effect on the α transition. By contrast, the presence of a DGEBA epoxy prepolymer size on T300 carbon fibres was said to be particularly noticeable, resulting in a resistance to relaxation assumed to be due to the formation of a more highly cross-linked, but less homogeneous network than that obtained with unsized fibres. A more detailed later study [11] on a wider range of fibres appears completely to reverse these conclusions, however. The introduction of untreated fibres resulted in an increase in the temperature of the α peak with increasing content of AU4 and AS4 fibres, but a decrease with increasing volume fraction, V_f, for T300 fibres, and the peak amplitude fell non-linearly with increasing V_f for all types of fibre. For oxidized fibres, an increased transition temperature and reduced peak amplitude indicated an increase in the rigidity of the interfacial zone due to improved fibre/matrix interaction, as also suggested by Chua [14] for glass/epoxy composites. Perret *et al.* [11] suggested that the oxidation treatment removes the weakly cohesive surface layers of the fibre and increases the concentration of functional groups which results in stronger fibre/matrix bonding and reduces molecular mobility in the interfacial zone. The presence of a size on the fibres, on the other hand, improves wetting but leads to a zone near the fibre surface deficient in catalyst in which the cross-link density is reduced as a consequence. The transition temperature is therefore also reduced and the peak amplitude increased. These effects are more marked the greater the volume fraction of fibres or the thickness of the coating, as would be anticipated.

Gérard [8] studied the effects of an elastomeric interphase in carbon/epoxy composites. The thicknesses of his coatings were of the order of 1% of the fibre diameter, and were therefore scarcely visible in the SEM. He observed that the α transition of the interphase was at approximately the same temperature as the β transition of the epoxide matrix, so that separation of the two was difficult. The introduction of oxidized or oxidized and coated fibres caused no changes in the characteristics of the β transition. By contrast, the temperature of the main relaxation peak fell by 2.5, 2.7 and 3.9 °C, respectively, for additions of uncoated fibres and of oxidized fibres with two levels of coating, suggesting higher degrees of chain mobility as the amount of surface elastomer increased. These changes were also accompanied by marked reductions in the apparent activation energy, but because the values quoted (799–940 kJ mol^{-1}) are far too great for molecular processes in a polymeric solid it is unclear what the significance of this might be. Gérard used the Cole–Cole approach, referred to earlier, modified with reference to a biparabolic model introduced by Huet [18] which extends Equation 3 to take account of the fact that complex plane plots of M'' versus M' for polymers are usually asymmetric, like the equivalent tan δ plots. This model gives the complex modulus as

$$M^* = M_R + \frac{M_U - M_R}{1 + (i\omega\tau_1)^{-h} + (i\omega\tau_2)^{-k}} \quad (4)$$

($0 < h, k > 1$), where h and k are parameters corresponding, respectively, to long times (low frequency, high temperature) and short times. Values of h and k, which are obtained from the right-hand and left-hand slopes of the Cole–Cole plot, were of the order of 0.5 and 0.2. Gérard showed that when carbon fibres were introduced into an epoxy network, the value of h, characterizing long times, decreased, while k, relating to short times increased slightly, showing a weak blocking of the molecular segments involved in relaxation by the interface. When carbon fibres with an elastomer coating were introduced into the resin, h increased, suggesting the presence of different chains in the network, while a simultaneous decrease in k indicated a reduction in the blocking of segmental motion at the interface when the coating was present. Both M_U and M_R fell when the level of surface coating was increased (again suggesting that the epoxy network was less cross-linked when fibres are added to the resin) and when the weight of the coating was increased.

DiBenedetto and Lex [19] also noted different effects of surface treatments in carbon and glass fibre composites, measurements of the interfacial shear strength suggesting that something appeared to happen at a glass/resin interface, but not at a carbon/resin interface, which caused the resin to be stronger at the fibre surface. Ide *et al.* [12], reporting an investigation of the dynamic response of unidirectional carbon/epoxy composites, comment that their polyacrylonitrile (PAN)-based fibre was used without de-sizing because they had noted that the presence of a sizing agent does not affect the mechanical dispersion of carbon-fibre-reinforced plastic (CFRP) materials. The tan δ peak for their bulk DGEBA matrix resin was at about 125 °C, and they observed that by increasing the carbon fibre volume fraction, the height of this primary peak was gradually reduced while secondary peaks of increasing strength developed at temperatures above 150 °C. They interpret their results to indicate that an interphase with a relatively strong interaction between the fibre surface and the epoxy matrix may exist, and that this interphase may consist of two kinds of phases with different properties.

In a paper dealing with glass/epoxy and carbon/epoxy composites, Thomason [13] warns of the possibility that artefacts may obscure the analysis of DMTA results. He summarizes the four reasons why the interfacial region may appear to have properties different from those of the bulk resin. These are:

(a) there may be a rigid polymer layer adjacent to the fibre surface caused by restricted molecular motion due to fibre/matrix interactions;

(b) there may be a zone next to the fibre that is different in composition from the bulk resin because of

preferential adsorption of one of the resin components;

(c) there may be a region next to the fibre that is different in composition from the bulk matrix because of incomplete dissolution of the fibre coating in the matrix resin;

(d) the layer next to the surface may have different mechanical properties because of residual stresses.

Thomason concludes that although it is often possible to obtain an apparent loss modulus peak, such as those described by Ide *et al.* [12], at temperatures higher than that of the α peak of the polymer matrix, this could be an artefact resulting from a combination of experimental factors. In his experiments he also obtained such higher temperature peaks, but he dismisses these as artefactual and shows that he was able to detect a true loss peak that could be ascribed to the presence of an interphase region, at temperatures substantially below the resin T_g, that was not resolvable by differential scanning calorimetry (DSC) methods. It is interesting to note that Williams *et al.* [20] determined directly the mechanical properties of the matrix surrounding the fibre in a single-fibre carbon/epoxy composite by means of a nano-indentor. They report that there is a soft interfacial zone, of the order of 500 nm thick, of which the modulus may be as low as a quarter of that of the bulk resin as a result of the fact that this region is depleted in amines. They also observe that measurement of the stiffness of this zone is affected by two opposing features, a mechanical stiffening of the interfacial zone because of the proximity of a rigid fibre, and the chemical softening due to the depletion in amines. It is not clear whether similar effects would be observed in real composites.

The amine depletion model was described by Drzal *et al.* [21] before the technique used by Williams *et al.* for studying the mechanical properties of the matrix close to the fibre became available. They pointed out that the amine concentration in the interphase close to the fibre surface would be below the stoichiometric amount necessary for full cure, and they support this hypothesis with data showing how the stiffness of a particular DGEBA resin rises as the amine concentration is reduced while, simultaneously, the fracture strength and fracture toughness of the resin decrease. These results indicate that the interphase should behave as a more brittle material than the stoichiometrically cured epoxy resin and Drzal *et al.* conclude that this should promote better stress transfer at the interface, resulting in a higher interfacial shear strength. Thus, the model of Drzal *et al.* appears to be somewhat at odds with the experimental measurements of Williams *et al.*, at least in relation to the supposed stiffness of the interphase layer. We note that Kardos [22], who has also detected interphase regions of this kind in glass/epoxy systems, specifically advocates the interpolation of an interphase of stiffness intermediate between the stiffnesses of the fibre and resin, because the consequent reductions of the modulus ratios between neighbouring phases must reduce stress concentrations.

Sellitti *et al.* [23] have also commented on the effect of surface treatment on the cure of the resin. They suggest that surface groups on the carbon fibres can act as catalysts for cross-linking and observe that in treated-fibre composites it is therefore possible to get either enhancement or retardation of curing depending on the nature and concentration of the surface groups. Finally, Grenier-Loustalot and Grenier [24] used a battery of methods, including nuclear magnetic resonance, Fourier-transform–infrared and DSC techniques, to show, with reference to results for pure epoxy resin, that the presence of glass and carbon fibres changes neither the cure reaction mechanisms nor the resin network structure, although it does change the cure reaction rate, depending on the surface treatment or coating which changes the reactivity of the prepregs. There is thus a marked divergence between the results of different groups of researchers in this field.

3. Experimental procedure

3.1. Fibres and surface treatments

The main fibre used in this programme was ENKA Tenax HTA-3000 fibre, a high-performance carbon fibre manufactured from polyacrylonitrile (PAN) precursor polymer, characterized as being a high-strength, standard-modulus fibre. Supplies of fibre provided by the manufacturer included samples without any surface treatment, samples that had been subjected to an oxidizing treatment, and samples that had been both oxidized and sized. Although no details of these commercial treatments are available it is likely that the oxidized and sized material would be that normally supplied for compatibility with epoxide resin matrices.

Samples of the fibre were subjected to a range of electro-polymerization and plasma polymerization treatments, the objective being to deposit a coherent polymer layer on the fibre surface that would act as an interphase when treated fibres were incorporated into resin-based composites. The purposes of such interphases as have already been widely studied are diverse, and include both modification of the chemical nature of the interfacial region, i.e. the wetting and the nature of the fibre/matrix bond, and amelioration of the stress state and conditions for stress transfer at the interface. The aim of our treatments was to lay down a thin polymer layer that would be rich in nitrogen-containing groups so as to improve the compatibility of the fibre surface with amine-cured epoxy resins. Full details of the experimental techniques used for these coating experiments and for studying the surface chemistry of the treated surfaces will be the subject of other papers from the Namur group. For the purposes of this paper, therefore, we simply summarize the treatments given and report the results of the X-ray photoelectron spectroscopy (XPS) studies of the fibre surface chemistry (Table I). The electro-polymerization treatments referred to in this paper were carried out on untreated fibres in a bath consisting of a solution of 0.1M *o*-diaminobenzene + 0.1M $LiClO_4$. The ep122 samples were treated for 20 min at 0.6 V,

TABLE I Summary of power-law curve fitting parameteres for epoxy resin and model carbon fibre composites. Fixed fitting parameters: $\tau_0 = 1.1 \times 10^{-11}$; $\alpha = 9$

Sample	Fibre orientation deg	Experimental data		Power-law parameters					
		T_α (K)	$(\tan\delta)_{max}$	T_0	A	m	n	Error (%)	r (degrees of freedom)
Resin		402	0.62	373.75	1.22	0.63	0.52	2.2	0.997(72)
Commercial treatments									
Untreated	90	403	0.58	375.34	1.10	0.63	0.63	2.5	0.995(33)
Oxidized	90	401	0.55	374.71	1.03	0.66	0.60	2.4	0.996(35)
Oxid/sized	90	403	0.59	375.64	1.10	0.67	0.64	2.5	0.995(32)
Untreated	0	401	0.42	373.12	0.81	0.70	0.43	2.3	0.995(34)
Oxidized	0	401	0.41	373.32	0.80	0.71	0.41	2.3	0.996(34)
Oxid/sized	0	401	0.41	373.46	0.81	0.70	0.45	2.4	0.995(34)
dip coatings									
PB	90	403	0.54	375.97	0.96	0.61	0.68	2.3	0.996(32)
PBA	90	403	0.60	376.34	1.06	0.63	0.70	2.2	0.996(33)
Latex	90	406	0.49	377.65	0.89	0.65	0.61	2.6	0.994(32)
PB	0	401	0.34	374.07	0.62	0.65	0.55	2.2	0.996(34)
PBA	0	400	0.38	371.46	0.64	0.60	0.54	1.9	0.996(34)
Latex	0	403	0.31	374.92	0.60	0.64	0.37	2.7	0.994(32)
ep and pp treatments									
ep122	0	401	0.35	373.72	0.65	0.66	0.55	1.9	0.996(37)
ep132	0	400	0.37	371.33	0.74	0.64	0.34	2.7	0.994(54)
pp3	0	400	0.39	371.79	0.75	0.67	0.51	2.0	0.997(58)

while the ep132 treatment was at 1.2 V for 10 min. The plasma polymerization treatment was carried out at a pressure of 0.1 torr (1 torr = 133.322 Pa) on oxidized/sized fibres in an acrylonitrile plasma for 60 min at 20 W plasma power.

3.2. Resin matrix

The resin used in this work was Ciba Geigy LY1927GB epoxy resin, a phenolic novolac resin containing about 7 epoxy equivalents/kg which is cured by 36 wt % formulated aliphatic polyamine hardener, HY1927GB. The DSC trace for a sample of the cured resin which is shown in Fig. 1 indicates that the glass transition temperature of the resin, T_g, is approximately 130 °C, or 403 K. The curing treatment, which was that recommended by the manufacturer, was as described in the next section.

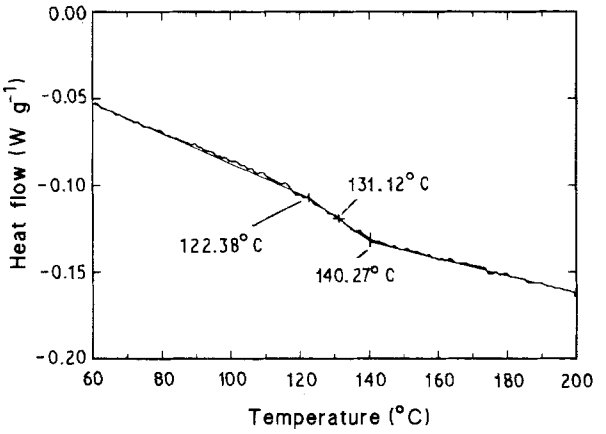

Figure 1 Differential scanning calorimeter trace for a sample of Ciba Geigy LY 1927 epoxy resin, cured as described in Section 3.3.

3.3. Test specimens

Model composites were prepared for DMTA analysis by impregnating short lengths of single tows of fibre with precatalysed resin, spreading them as uniformly as possible on to a Melinex sheet on a glass plate, and then flattening them by laying another plate on top. The thickness of the samples was held at about 1 mm by interposing microscope slides between the two glass plates. The assemblies were allowed to gel overnight at room temperature, and then given an initial cure of 2 h at 60 °C, a final cure of 2 h at 80 °C, and a post-cure of 24 h at 100 °C. The resulting samples were cut into test pieces of dimensions 30 mm × 10 mm and the surfaces of these specimens were ground to remove excess resin or other shallow surface defects. The edges were also ground flat and parallel, and the samples were then dried overnight in a desiccator prior to testing.

Three groups of test samples were prepared. The first of these was an exploratory group containing the fibres supplied by the manufacturer, namely those in the untreated, oxidized, and oxidized/sized conditions, together with samples of the plain resin. The second was a group containing the fibres treated by electro-polymerization (ep122 and ep132) and plasma polymerization (pp3) (the designations refer to the treatments discussed in our earlier paper [1]).

The third group of samples was a comparator group which was prepared before the availability of experimental quantities of the electro-polymerization or plasma polymerization treated fibres. A number of samples were prepared from fibres coated by solution-coating with an elastomeric polymer. This was accomplished by dipping tows of untreated fibres into a

water-based emulsion of polyisoprene (latex), into polybutadiene (PB) dissolved in cyclohexane, and into poly(butyl acrylate) (PBA) dissolved in acetone. The latex was a commercial BF Goodrich "Hycar" latex emulsion which was diluted to form a 10 wt % solution. The PBA solution contained 1% of the polymer by weight, and the PB 2%. These solutions were selected for convenience of handling by simple dipping methods. Sufficient tows to fill a mould were dipped into the solutions and spread as much as possible to facilitate penetration. The bundles were subsequently dried and laminated into model composites, as in the case of the commercially treated fibres. The approximate thicknesses of the coatings applied were estimated to be 0.2 μm for the latex, and 0.03–0.04 μm for the PB and PBA. These comparator samples were made from Courtauld Graffil HMU untreated carbon fibres, and it is interesting to note that although two different types of fibre were used in this work, there was no DMTA evidence of any difference between the composites containing the two species of fibre.

For the commercially treated fibres and the dip-coated samples, sufficiently large specimens could be made to permit test strips to be cut at 0° and 90° to the fibre direction in order to assess the effect of fibre orientation on the dynamic elastic response. For the electro-polymerization and plasma polymerization coated fibres, however, the quantities available were only sufficient to permit the preparation of test samples with axially aligned fibres. The fibre volume fractions achievable in the ep122, ep132, and pp3 specimens were 0.20, 0.16 and 0.22, respectively, somewhat higher than that achievable with uncoated fibres for which the volume fraction was only 0.1.

3.4. Dynamic mechanical analysis system

The system used in this work was the Polymer Laboratories DMTA Mark II equipment which has the capability of analysing samples over the temperature range −150 to +300 °C at frequencies from 0.01–200 Hz. Its temperature resolution is 0.1 °C, and it is equipped with a high-duty bending head which provides information about the flexural properties. The temperature and frequency range encompasses most of the important primary and secondary molecular processes in conventional polymers, including the β and γ processes due to restricted chain or side group motion in addition to the main T_g and T_m transitions. It should be pointed out that the value of the room-temperature storage modulus for a plain resin sample determined by this equipment does not coincide with the conventional value of the tensile Young's modulus, E. As a result partly of the gripping method, partly of the sample geometry, and partly of the flexibility of the samples, the stiffness value determined is some combination of the extensional, compression and shear moduli, and, in consequence, is well below the normal value of E of about 3 GPa. In presenting the results of this work, however, we shall follow the normal practice of using the symbol E for modulus, and because all of the moduli of a viscoelastic solid exhibit the same temperature and frequency characteristics, the discussion of tan δ in Section 5 is unlikely to be unaffected by the discrepancy referred to above.

The Polymer Laboratories dual cantilever sample testing arrangement was used and the normal strain level applied to the specimen in bending corresponded to a nominal peak-to-peak displacement of 16 μm. Because of the high stiffness of some of the composite samples, however, some experimental runs were necessarily at constant power rather than constant displacement. Liquid nitrogen was used as the cooling medium, and following stabilization at the lowest temperature chosen for a given run, scans were carried out at a heating rate of 2 °C min^{-1}. Temperature scans were usually carried out from −80 to +200 °C at a frequency of 1 Hz, but detailed analysis of the results was mostly restricted to the region of the main loss peak, the α peak, associated with the glass transition. Experimental values of storage modulus, E', loss modulus, E'', and viscoelastic damping, tan δ (i.e. E''/E'), are stored as digital data for plotting by the DMTA machine and these were subsequently accessed for more detailed data analysis by methods not provided by the commercial DMTA software.

4. Results

Graphs of storage and loss moduli (on logarithmic scales) versus temperature for the plain resin and for composites with untreated, oxidized and oxidized/sized fibres are shown in Figs 2 and 3. All of the graphs have the same shape, exhibiting a single major (α) peak at about 130 °C, unexpectedly close to the DSC T_g value of 130 °C referred to earlier, and a broad, weakly defined β transition in the region of 50 °C. In both the 0° and 90° fibre orientations the E' and E'' curves for the three fibre composites are closely bunched and separated from the equivalent curves for the plain resin by amounts which reflect the level of fibre dominance of the elastic properties. There is a certain

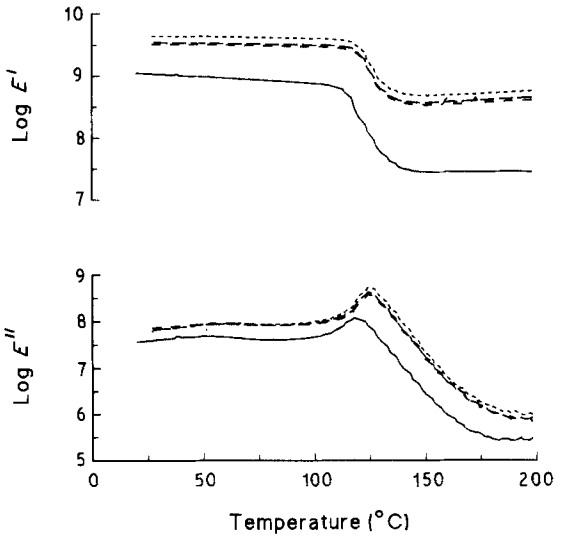

Figure 2 Storage and loss moduli, E' and E'', for model composites containing samples of (———) untreated, (– – –) oxidized, and (- - -) oxidized and sized Enka HTA fibres in (——) Ciba Geigy LY 1927 epoxy resin. The fibre orientation is 0° with respect to the sample length. Graphs for the plain resin are also included.

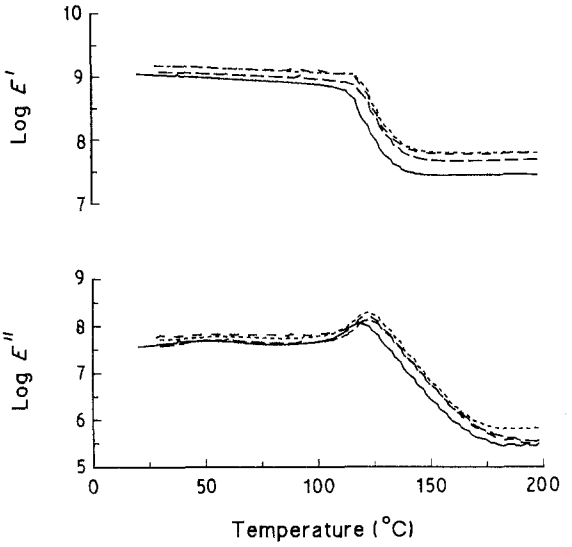

Figure 3 As for Fig. 2, but for fibre orientations of 90° (i.e. transverse).

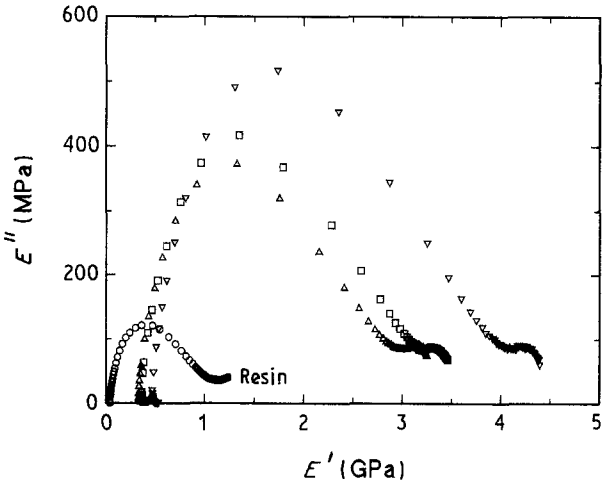

Figure 4 Cole–Cole plots of loss modulus versus storage modulus for plain epoxy resin and model composites containing (□) untreated, (△) oxidized, and (▽) oxidized/sized Enka HTA carbon fibres. Fibre orientation is 0°.

degree of overlap of the composite curves, although it is clear from Fig. 2 that the oxidized/sized fibres yield the highest overall composite stiffness, E', and also the highest loss modulus in the region of the peak and above.

Fig. 4 shows Cole–Cole plots for the plain epoxy resin and for model composites (0° fibre orientation) containing untreated, oxidized and oxidized/sized fibres. There is the same marked difference between the resin and composites as that shown by Gérard [8], but by contrast with his work, there is no apparent difference in the values of either h or k with fibre surface treatment and the value of k for the resin is markedly lower than those for the composites. No comment can be made about the relative values of E_U and E_R because of differences in fibre content. Although not shown, we note that the Cole–Cole plots for the plain resin and the untreated fibre composite with fibres at 90° to the loading direction were very similar in shape and magnitude, although the k value for the composite was somewhat higher. Fig. 5 shows Cole–Cole plots for the two groups of treated fibre composites (all in the 0° orientation) together with curves for the untreated fibre composite for comparison. For the lower group of dip-coated fibres there is a perceptible but small increase in the value of k through the sequence untreated, latex-coated, PB-coated, PBA-coated, while h remains unchanged. By contrast, for the electro-polymerization and plasma polymerization treated fibres, there are no observable differences in either h or k with surface treatment.

Because the mechanical loss, tan δ, is the ratio of the loss modulus to the storage modulus, the loss tangent is therefore a self-normalizing parameter with respect to differences in specimen stiffness. This means that an analysis of the differences between composites with different surface treatments where it has not been possible to maintain the fibre volume fraction constant from sample to sample is more sensibly made with reference to tan δ than to the loss modulus, E''. Some of the differences between treatments suggested by Figs 2 and 3 will not, therefore, necessarily be

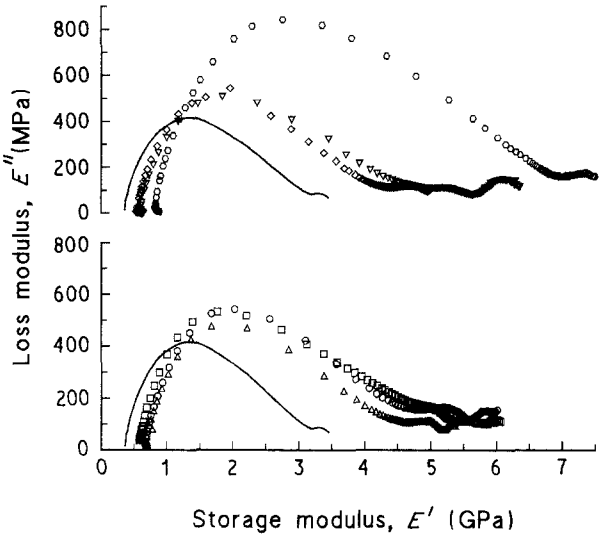

Figure 5 Cole–Cole plots for model composites containing untreated and surface-treated carbon fibres. In the lower group the fibres were dip-coated, while the upper group includes electro-polymerization and plasma polymerization treated fibres. (——) untreated, (▽) ep 122 coating, (◇) ep 132, (⬡) pp 3, (○) PB coating, (□) PBA, (△) latex.

transferred to curves of tan δ versus temperature. This is shown by Fig. 6a in which the tan δ data points in the region of the glass transition are shown for the plain resin and for model composites containing untreated fibres in the 0° and 90° directions. It can be seen that there is very little difference between the data for the resin and the 90° composite, the peak height being reduced by about 7%, from 0.62 to 0.58, and many of the data points overlappping. For the 0° orientation, by contrast, the peak height is reduced by 32% to 0.42. The reduced loss in the composite with 0° orientation is presumably a result of the fact that in this orientation the very much stiffer fibres control the deformation so that the more lossy component of the composite, assumed to be the interphase/interface, is less highly strained.

The shape of the curve and its position are not much altered, although because of the spacing of the

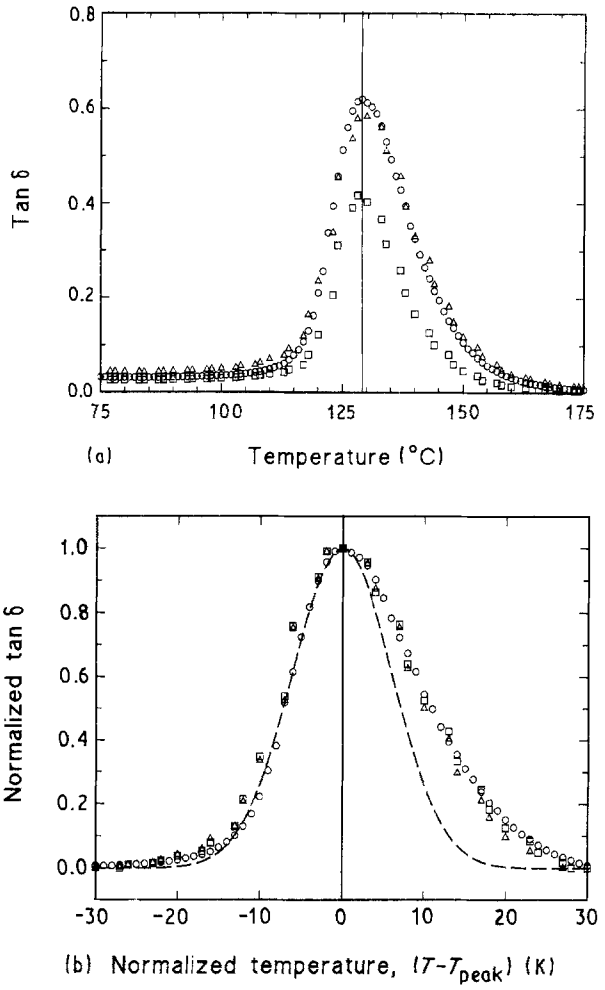

Figure 6 (a) Damping (tan δ) peaks for (○) LY 1927 resin and model composites containing untreated Enka HTA fibres in the (□) 0° and (△) 90° orientations. (b) Normalized tan δ curves for (○) plain LY 1927 epoxy resin and model composites containing (□) untreated, and (△) oxidized and sized Enka HTA carbon fibres. (– – –) A normal distribution curve drawn so as to fit reasonably closely to the lower temperature side of the resin peak. Fibre orientation = 90°.

data points it is not possible to determine, to within two degrees or so, the precise position of the maximum. The problem of analysing loss peaks to show the differences brought about by fibre surface treatments may be seen by normalizing the tan δ data for the plain resin and for the 90° composites containing untreated and oxidized/sized fibres. Fig. 6b shows the data for these materials normalized with respect both to peak height and peak temperature. The three sets of data coincide to a very large extent, and it can be seen from the Gaussian distribution curve imposed on the data points that all three curves are asymmetrical. The data appear to be largely superimposed, and give no clear indication at this level of analysis of the presence or absence of any interphase.

By contrast, the loss curves for the dip-coated fibre composites show rather more distinctive features, as illustrated in Fig. 7. Again with the proviso that exact location of the maximum is uncertain, it can be seen that there are differences in both peak height and peak temperature between the three samples, and there are also marked differences in the shapes of the curves below the α transition.

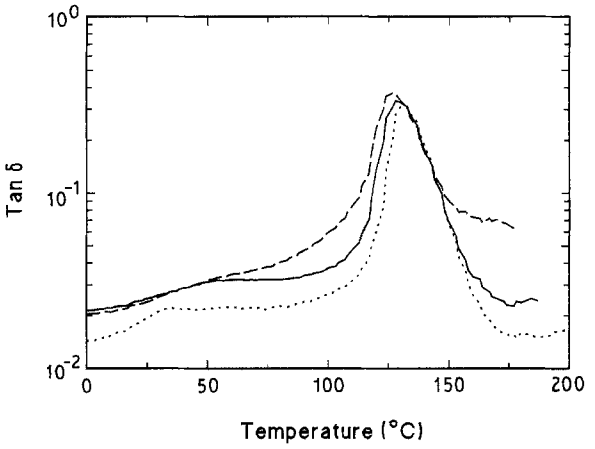

Figure 7 DMTA tan δ curves for model composites consisting of carbon fibres coated with (——) polybutadiene, (– – –) poly(butyl acrylate), and (. . .) latex in LY 1927 epoxy resin. Fibre orientation = 0°.

5. General discussion

Raw DMTA data for a range of samples may be compared, as we have seen, in terms of such obvious parameters as loss peak height, $(\tan\delta)_{max}$, and peak temperature, T_α, but these parameters do not permit the differentiation of very subtle changes in the character or shape of the peak. They may also give excessive weight to single data values, especially if the data points near the maximum are well spaced. A better method is to find an appropriate function the parameters of which may be systematically studied as functions of particular variables, such as interfacial shear strength. For the plain LY1927 epoxy resin used in this work we have developed a power-law function which gives good predictions of the temperature and frequency dependences of tan δ, and this is an appropriate starting point for analysis of the present results.

5.1. Power-law analysis

In a polymer in the vicinity of the glass transition the applicability of Equations 1 and 2 is questionable. The reason why the mechanical loss peak is observed at a temperature a little above the glass transition temperature is that in this temperature range elastically coupled entities within the polymer "slow down" to a natural relaxation rate matching the low applied frequencies. This "slowing down" is not correctly described by the simple Arrhenius expression of Equation 2. Moreover, in this temperature range polymer components become strongly interacting and it is known [25] that relaxation processes become non-exponential, whereas a simple exponential decay process is assumed in the derivation of the Debye expression of Equation 1a.

Although the conventional Arrhenius expression, Equation 2, is often invoked to characterize DMTA data for polymers, the activation energies and attempt frequencies are, in many quoted cases, unphysically large. We have shown [26], for example, that for the epoxy resin used in this work the apparent activation energy was 4.4 eV and the "attempt frequency" 1.7×10^{38} Hz. The latter is ridiculously large considering

that the highest frequency possible in the material is the atomic vibrational frequency which is bound to be in the range 10^{12}–10^{14} Hz. In addition, it is well known that the temperature-dependence of viscosity, and consequently the relaxation time, in a polymer are not accurately represented by an Arrhenius relationship. The Vogel–Fulcher law, a simple modification of the Arrhenius relationship, provides a much improved fit to experimental data. The corresponding expression for relaxation time is

$$\tau = \tau_0 \exp [E_a/k(T - T^*)] \quad (5)$$

in which T^* is a reference temperature which is obtained by fitting data. T^* is usually only a few tens of degrees below the glass transition temperature, T_g, and as a consequence both E_a and τ_0^{-1} adopt much smaller and more realistic values than necessary for the Arrhenius expression.

Williams *et al.* [27] showed from an analysis of a wide range of polymers that the temperature dependence of the ratios of mechanical relaxation times conformed to a universal empirical function

$$\log_{10}(a_T) = -8.86\,(T - T_s)/(101.6 + T - T_s) \quad (6)$$

in which a_T is the ratio of the relaxation time at a temperature T to that at a reference temperature T_s, recommended to be about 50 K above T_g.

A more recent alternative, investigated by Souletie and Thoulence [28] for the paramagnetic susceptibility of spin glasses, is to treat the slowing down in the same way as the critical slowing down that occurs in the vicinity of a true phase transition. Phase transition theory has received an enormous amount of attention in recent years and the value of scaling relationships is widely accepted. The dynamic scaling near a transition at T_0 should ideally follow a power law [29]

$$\tau = \tau_0[(T - T_0)/T]^{-\alpha} \quad (7)$$

where $\alpha = z\nu$ and ν is the critical exponent of the correlation length and z is the dynamic exponent.

Turning to the problem of the mechanical relaxation response function, Equation 1, the discrepancy between the prediction of the classical Debye expression and experimental data is typical of both the mechanical and dielectric responses of polymers and a wide range of other materials. Traditionally [2], this was dealt with by postulating a distribution of relaxation times, each contributing a relaxation peak and thus accounting for the much broader peak than that attributable to a single relaxation time process. However, there is now considerable doubt about the validity of this procedure because it implicitly assumes each relaxation process to be exponential. As mentioned above, non-exponential relaxation characterizes the dynamics of polymers, particularly near T_g, and there is an extensive body of theoretical work [25] that accounts for these non-exponential relaxations. Much of this arrives at the experimentally derived "stretched exponential" sometimes called the Kohlrausch or Williams–Watts function

$$f(t) = \exp[-(t/\tau)^n] \quad (8)$$

where the exponent n has a value between 0 and 1. Jonscher [30, 31] has developed a somewhat more adaptable function for fitting to the dielectric loss data of polymers. The function may be adapted to provide an expression for tan δ of the form

$$\tan\delta = A[(\omega\tau)^{-m} + (\omega\tau)^{1-n}]^{-1} \quad (9)$$

with two exponents, m and n, which enable the low and high $\omega\tau$ slopes of an absorption peak to be fitted separately, $\omega/2\pi$ being the test frequency, 1 Hz for the experiments reported here. The parameter A is a scaling factor related to the tan δ peak height which is determined by the modulus function B in Equation 1b. The expression for tan δ reverts to a Debye function on setting $n = 0$ and $m = 1$ [26]. Thus, the full power-law expression for tan δ as a function of temperature is:

$$\tan\delta = \frac{A}{[\omega\tau_0(1 - T_0/T)^{-\alpha}]^{-m} + [\omega\tau_0(1 - T_0/T)^{-\alpha}]^{1-n}} \quad (10)$$

We note that reducing T_0 in Equation 10 shifts the whole curve to the left, lowering the peak temperature without changing the shape or the peak height. Raising τ_0 pulls the curve to the right, again leaving the height unaffected, but maintains the same left-hand start point if T_0 remains unchanged. If both T_0 and τ_0 remain fixed, raising m steepens the right-hand wing of the curve while raising n steepens the left-hand wing, in both cases causing simultaneous downward shifts in the peak temperature and small increases in peak height. Thus, it is possible that in a series of experiments such as we have described, the fundamental behaviour of the polymer matrix, as determined by α and τ_0, could be expected to remain unchanged while subtle effects due to surface treatments, for example, may be mapped by variations in T_0, A, m and n. For reference, Fig. 8 illustrates these more obvious effects of the power-law parameters on loss-peak appearance starting with a data set that represents the plain resin response.

5.2. Analysis of DMTA loss-peak data

Equation 10 is an asymmetric function which falls to a common base-line on each side of the peak. The raw data shown in earlier figures must therefore be modified before the power-law curve can be fitted. In principle, this would require a deconvolution process to subtract what is effectively a very broad and flat "peak" to the left of the main α peak, but it can be done with little error by a linear subtraction process to bring the left- and right-hand wings of the tan δ curves to a common (zero) base-line. This modification is of trivial consequence in that it does not markedly alter the peak height or position. The fitting was carried out with the aid of a non-linear regression algorithm provided by the graphing package **Fig. P** marketed by Biosoft of Cambridge, UK. Refinement of the fitting procedures reported in our earlier paper [26] pro-

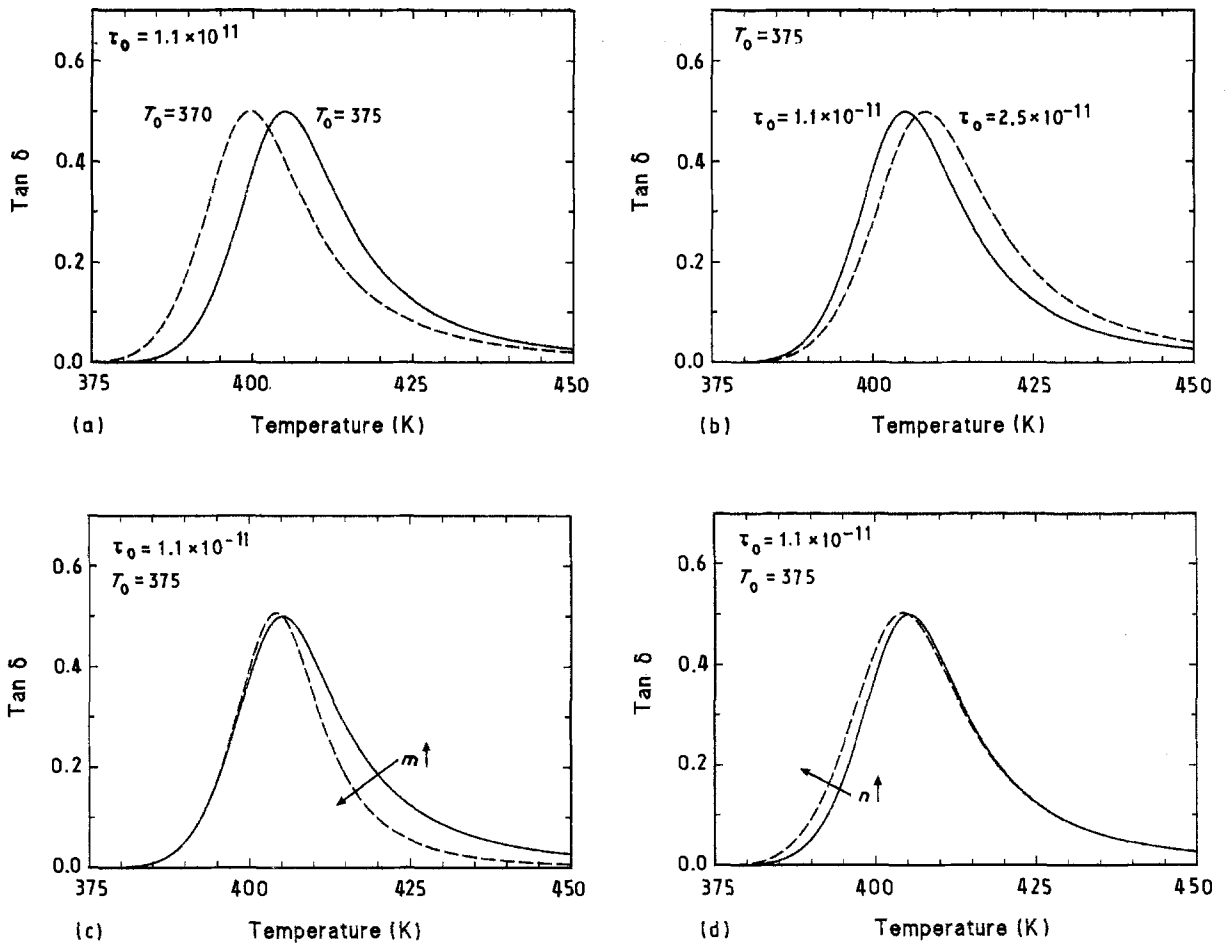

Figure 8 Illustrations of the effects of the power-law parameters on the shape of the modelled tan δ versus temperature curve in the vicinity of the damping peak. (a, b) $A = 1.0$, $m = 0.5$, $n = 0.5$; (c) $A = 1.0$, $m = 0.7$, $n = 0.5$; (d) $A = 1.0$, $m = 0.5$, $n = 0.6$.

vided a set of fitting parameters for the plain resin, i.e. $T_0 = 373.75$ K, $\tau_0 = 1.1 \times 10^{-11}$s, $\alpha = 9$, $A = 1.22$, $m = 0.63$, and $n = 0.52$, which were marginally different from those given in our earlier paper [26] but which were in somewhat better agreement with the background arguments presented in the paper. They were reproducibly obtained by refitting repeatedly from different starting values of the parameters. The values for τ_0 and α were then retained as constants and the fitting procedure repeated for all of the composite samples in order to determine T_0, A, m and n. The results are presented in Table I. An indication of the goodness of fit was obtained in each case by determining the mean absolute deviation of the fitted curve from each data point. These errors are reported in Table I as a percentage of the peak height, $(\tan \delta)_{max}$, and it can be seen that they are all of the order of 2%. The curve-fitting programme also provides an indication of the standard error for each of the fitted parameters. The accuracy of fitting for T_0 was found in each case to be of the order of only 0.5 K, rendering its value much more sensitive as an indicator of the glass transition temperature than the experimentally observed value of the temperature at which the largest value of tan δ occurs, for reasons referred to earlier. The values of A, m and n were fitted with errors within the range 0.01–0.04, but these were mostly clustered around 0.03. The reported correlation coefficients, r, also given in Table I were all 0.994 or higher, for degrees of freedom ranging between 32 and 58.

From the tabulated results, it can be seen that the estimated values of the peak temperature, T_α, are almost all within a couple of degrees of each other, but fall into two groups. It appears that whereas the values for the plain resin and the model composites of 90° orientation are mainly near to 403 K, those for the 0° orientation are by and large nearer to 400 K. Only the composites with the latex-coated fibres seem not to fit this pattern, both of these giving noticeably higher T_α values than their respective group averages. The table also shows that the variations of the fitted power-law parameter, T_0, seem to follow the same pattern as that described above for T_α.

The values of the peak height parameter, A, are also noticeably different for the two orientations. The 90° composites give values near to unity, compared with 1.2 for the plain resin, while the values for 0° composites themselves fall into two groups, about 0.8 for the commercial treatments and 0.6–0.75 for the experimental treatments. The latex-coated fibre samples, with the thickest of all the coatings studied, provide the lowest values of A in the respective 0° and 90° groups, and the 0° dip-coated samples give the lowest peak heights overall. This is in marked contrast to the findings of Chua [14, 15], referred to earlier, which indicated that the peak height increased with increasing coating thickness. The curve shape parameters, m and n, show some variation between groups of results, but it can be seen that it is mainly n, the exponent describing the shape of the low-temperature side of the

curve, that is most sensitive to surface treatment, m remaining mostly in the range 0.6–0.7.

A typical set of results, from which some of the data in Table I were obtained, is shown in Fig. 9. This includes the experimental data for the shapes of the α peaks for composites with untreated, oxidized, and oxidized/sized fibres in both the 0° and 90° orientations, together with the fitted power-law curves. For reference, the fitted curve for the plain resin is also given with each pair of data sets. The figures confirm the similarity of the shapes of all of these curves, the very small peak temperature shifts (0° composites and plain resin marginally lower than 90° composites), and very slight differences between the curves for different fibre treatments. These results certainly do not suggest that there is any marked effect of the fibre surface on the curing of the epoxy resin, and appear to be in agreement with the work of Garton *et al.* [17] and Grenier-Loustalot and Grenier [24]. It can also be seen, from a comparison of the three sets of data in this figure that the presence of an epoxy-compatible size on the fibre surface appears to have little influence on the nature of the cured resin layer near the interface.

Fig. 10 shows the results of fitting the power law to the tan δ data for the electro-polymerization and plasma polymerization treated fibres in the 0° orientation. As in the case of the commercial treatments, the visible differences in the three sets of data are not very marked, but whereas the curve for the ep 122 treatment is similar in shape and position to that for the untreated fibre sample, the ep132 and pp3 treatments appear to shift the curve increasingly to the left. For comparison, the family of curves for the dip-coated fibres, again in the 0° orientation, are shown in Fig. 11. Here, the polybutylene curve can again be seen not to be displaced from that of the untreated sample, but the other two treatments appear to cause effects of an opposite nature. The PBA treatment shifts the curve to the left, as in the case of the plasma polymerization treatment, whereas the effect of the latex coating is to shift the curve to the right, the effect being more marked than those of any other treatment represented in this work.

Table I shows that the derived values of T_0 for all samples in the 0° orientation are very similar and close to that for the plain resin, the mean value being 373.02 K, with a standard deviation of 1.24 K, compared with 373.75 K for the plain resin. The values for the ep132 and pp3 treatments appear to give the lowest values of T_0 (although by only a degree or so), and we note that these treatments were shown, in our earlier paper, to deliver the highest interfacial shear strengths of a substantial group of experimental treatments [1]. It is interesting, therefore, to attempt to correlate some of the power-law parameters with interfacial shear strength. Values of τ_i are given in [1] only for the commercial treatments (ut, ox, and ox/sz) and for the experimental treatments ep122, ep132 and

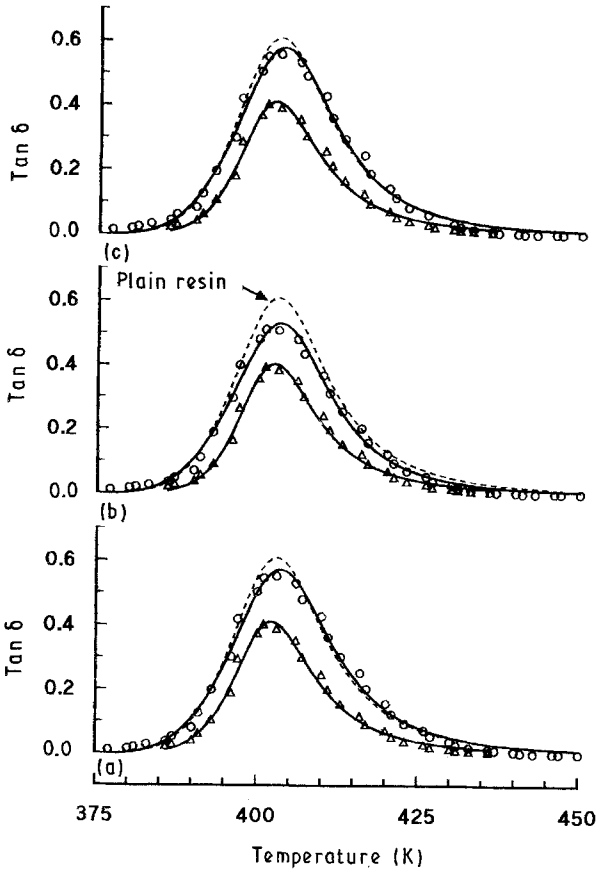

Figure 9 Power-law model fitted to experimental tan δ versus temperature curves for model composites containing (a) untreated, (b) oxidized, and (c) oxidized/sized carbon fibres. (△) 0° fibre orientation; (○) 90° orientation; (– – –) fitted curve for the plain LY 1927 epoxy resin.

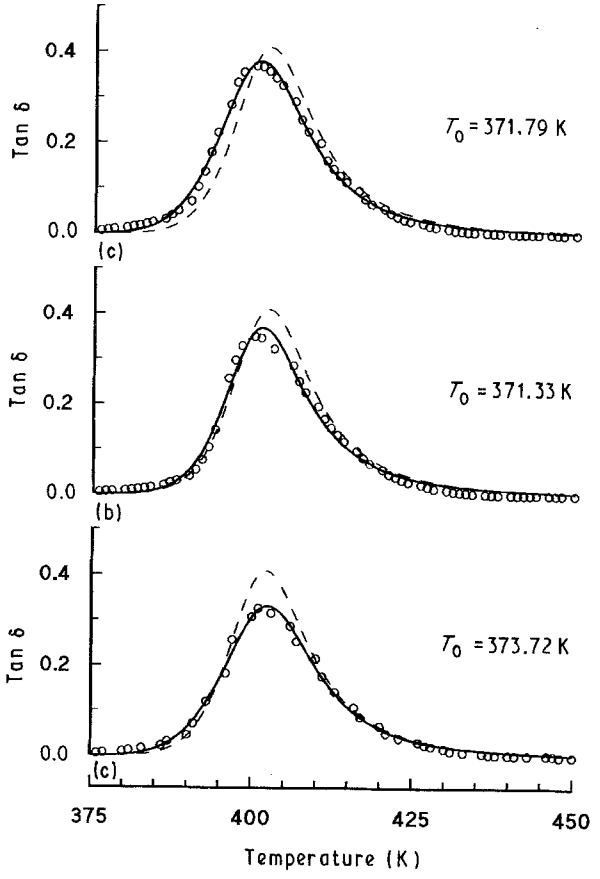

Figure 10 Power-law model fitted to experimental tan δ versus temperature curves for model composites containing carbon fibres with treatments (a) ep122 and (b) ep132 (electro-polymerization) and (c) pp3 (plasma polymerization). Samples were tested in the 0° fibre orientation: fixed parameters $\alpha = 9$, $\tau_0 = 1.1 \times 10^{-11}$. (– – –) The fitted curve for the untreated fibre composite.

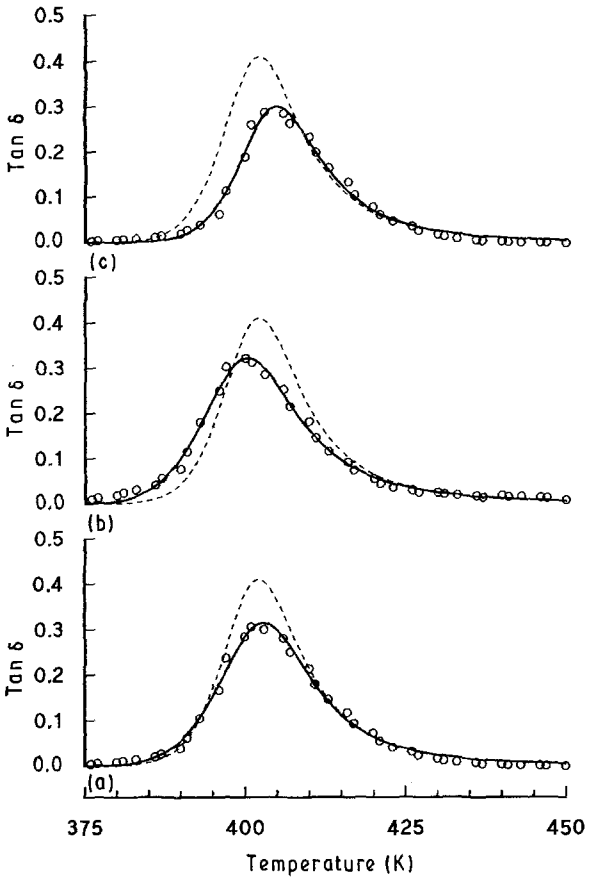

Figure 11 Power-law model fitted to experimental tan δ versus temperature curves for model composites containing carbon fibres coated with (a) polybutylene, (b) poly(butyl acrylate), and (c) latex. Fibre orientation = 0°: fixed parameters $\alpha = 9$, $\tau_0 = 1.1 \times 10^{-11}$. (– – –) The fitted curve for the untreated fibre composite.

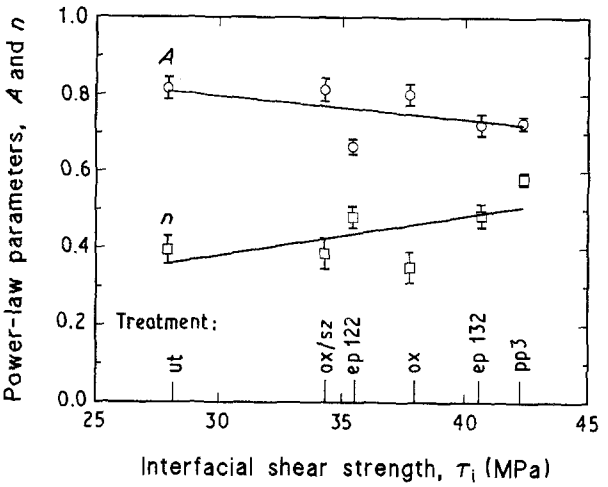

Figure 12 Correlation between power-law parameters A and n and the interfacial shear strength, τ_i. The constant parameters used in the power-law fit were $T_0 = 372.79$ K; $\alpha = 9$, $\tau_0 = 1.1 \times 10^{-11}$. The error bars shown are 95% confidence limits for the power law fits.

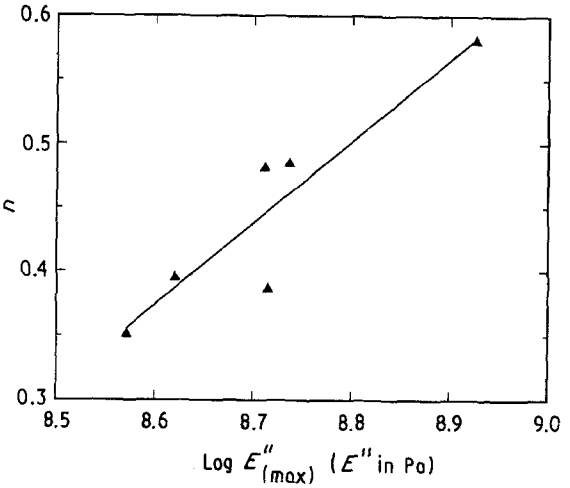

Figure 13 Relationship between the power law exponent, n, and the peak value of the loss modulus (log scale).

pp3. Because it appears likely, from Table I and the curves of Figs 9–11, that the scaling parameter A and the exponent n are the parameters most likely to be affected by the treatments, we have simplified the situation by refitting the data with the reference temperature, T_0, also held constant at the mean value for the group of samples under discussion, i.e. 372.79 K (i.e. excluding the data for the dip-coatings for which τ_i values are not available). The effect of fixing T_0 in this way makes no perceptible difference to the accuracy of fit, but it changes the values of A, m and n slightly from those given in Table I. We have already seen that m varies little with treatment but, as Fig. 12 shows, there is some evidence that A falls slightly as the interfacial shear strength is increased, while the value of n increases rather more markedly over the same range. The error bars indicated in this diagram are the 95% confidence limits returned by the curve-fitting programme for the fitted values of A and n: we should also note, however, that the likely uncertainty in determining the value of τ_i from single-filament strength tests and single-fibre-composite fragmentation tests is, as discussed in [1], of the order of 25%. The regression equations represented by the two lines in Fig. 12 have slopes -0.006 (for A) and $+0.0103$ (for n), the units of τ_i being MPa, and their respective correlation coefficients are -0.498 and 0.625 for 10 degrees of freedom. We note that the corresponding tabulated values of r at the 90% and 95% confidence levels are 0.497 and 0.576, respectively. Thus, the single power-law parameter that is most strongly correlated with the direct effect of surface modifications on the interfacial shear strength appears to be the parameter n describing the lower temperature (or higher frequency) side of the tan δ curve, effectively the equivalent of k in the Huet analysis of Equation 4. Neither the modified peak height, A, nor the temperature at the α peak maximum show such a strong response as that of the exponent n. As described earlier, Gérard showed that the Huet parameter h, which characterizes long relaxation times (or high temperatures), increased when carbon fibres with a flexible coating were added to epoxy resin, suggesting the presence of different chains in the network. But he also noted a reduction in k, which he considered to indicate a reduction in the blocking of segmental motion at the interface when the coating was present. As we have seen, the effect of surface treatments on m (the equivalent of the Huet h) is very slight indeed, and even in the presence of the thicker dip-coated fibres m shows no variation. We note, for

reference, that there appears to be a strong relationship between the power-law exponent n and the logarithm of the absolute maximum value of the loss modulus, E'', as shown in Fig. 13 ($r = 0.918$; 10 degrees of freedom).

6. Conclusion

It is clear from the review in Section 2.1 that there are some contradictory aspects of our state of understanding of the nature of the interfacial region in composites and its effect on the dynamical mechanical response, and previous research does not guide us to a simple interpretation of the experimental results presented here.

For the surface treatments investigated, it can be seen that the experimental parameters obtained from DMTA analysis which show some sensitivity to the surface modification are the loss peak temperature, T_α, (and the related power law characteristic temperature, T_o), the peak height, $(\tan \delta)_{max}$, (and the related power-law A parameter), and the power-law exponent n, which relates to the shape of the lower-temperature wing of the loss peak. The power-law parameters have the advantage that they can be more accurately defined than the related values estimated from the original experimental data.

T_α and T_o both fall slightly, by two or three degrees, with oxidation, electro-polymerization, and plasma polymerization treatments, and increase slightly, again by a degree or so, with the thicker dip-coatings. The patterns of variation of A and n are not very definite, but there is some reasonable indication that A (the peak height) falls slightly as a result of treatments that increase the interfacial shear strength, τ_i, while n (indicating a downward displacement of the left-hand wing of the peak) rises somewhat erratically with increasing τ_i. These observations relate to the oxidation, electro-polymerization and plasma polymerization treatments only, because no shear strength measurements were made for the dip coatings. An increase in n and a fall in T_o are both associated with a lowering of the peak temperature, but occurring together, without a simultaneous change in m, they suggest an associated slight broadening of the peak and a modest reduction in thermal stability. Only the composite with the thicker latex dip-coated fibres showed a clear indication of a raised loss peak temperature, indicating a difference in character between this interphase and the type of interphase/interface present in composites representing all other surface treatments.

There is some evidence of fibre orientation effects. For those groups of samples where DMTA tests could be carried out at both 0° and 90° to the fibre direction, both T_o and A are lower in the axial direction than in the transverse direction. As we have said earlier, because A is effectively normalized with respect to overall composite stiffness, we would not necessarily expect it to vary with fibre orientation. But because the test geometry involves a complex stress situation, with unknown contributions from the different composite stiffness components, it is not possible to be certain about whether there is genuinely a lower mechanical loss in the 0° orientation. If, on the other hand, there is a compliant interphase whose presence is revealed by a slight lowering of the peak temperature, one might expect its effect to be more marked in the transverse orientation than in the fibre-dominated direction. However, if we suppose that in the 0° three-point bend test orientation shear in the matrix and interphase is the dominant source of loss, but in the 90° orientation the interphase is predominantly loaded in triaxial tension, one might then expect to detect a higher level of mobility in the 0° orientation.

It can be seen from Fig. 12 and Table I that the observed shifts in these power-law parameters are very small given that the increase in τ_i involved is nearly a factor of 2. The small changes do not suggest the occurrence of such important modifications to the polymer structure in the interface region as those suggested by some of the workers whose results have been referred to earlier. We have already shown [1] that the observed changes in τ_i are also only very weakly related to surface nitrogen content. Chua [14, 15] and Jang [32] have also shown an inverse correlation between peak height and bond strength, but to a greater degree than that shown by our results. The associated small downward shift in the peak temperature, of the order of two or three degrees for ep 132 and pp3, is similar to the shifts reported by Gérard [8] and conforms to the ideas of Thomason [13].

Various workers [9, 10] have suggested that the presence of an interphase should result in an increase in the tan δ peak height, but none of the present results show any indication of this, and indeed the composites with the thickest polymer coatings produced by dipping had relatively low A values. Because, in these experiments, there is no apparent difference in behaviour between the composites containing fibres with an epoxy-compatible size and those with untreated or non-sized treatments, it is also difficult to see how the Drzal stiff/weak depleted-amine interphase model could apply. The present results are also completely at odds with those of Ide *et al.* [12], because we find no evidence of a second higher-temperature loss peak when fibres are introduced.

In general, the results for plain resin and composites are in agreement with the ideas of Garton *et al.* [17] and Grenier-Loustalot and Grenier [24], namely that the presence of a carbon fibre surface, whether treated or untreated, affects neither the resin cure reaction nor the resin network structure.

The DMTA loss peaks in these composites have been accurately fitted by means of a non-Arrhenius power-law expression for the temperature dependence of the relaxation time, and there is evidence that the effects of some surface treatments can be detected and the value of interfacial shear strength, τ_i, correlated with two of the parameters of this power law, namely, the peak height parameter, A, and the exponent n which characterizes low-temperature (high-frequency) events. There are some similarities between this power-law model and the Huet development [18] of the Cole–Cole model [3] for dielectric behaviour in

which an exponent k, which also characterizes low-temperature events shows changes as a result of fibre surface coating treatments [8].

There is considerable evidence to support the conclusion that the effects of experimental surface treatments on τ_i are not as simply related to the viscoelastic characteristics of the interface or interphase as has often been suggested.

Acknowledgements

This study is part of a wider programme on surface treatment of carbon fibres for composite materials carried out jointly in the Facultés Universitaires Notre-Dame de la Paix, Namur, Belgium, and the School of Materials Science, University of Bath, UK. We are grateful to the EEC for its financial support and to "Enka" for the supply of carbon fibres. The experiments on the dip-coated fibres were carried out by Mr A. K. Man as a final year student project at Bath.

References

1. B. HARRIS, O. G. BRADDELL, C. LEFEBVRE and J. VERBIST, (1992), Plastics, Rubber and Composites, Processing and Applications, **18**, 221–240.
2. N. G. McCRUM, B. E. READ and G. WILLIAMS, "Anelastic and Dielectric Effects in Polymeric Solids" (Wiley, London, 1967).
3. K. S. COLE and R. H. COLE, *J. Chem. Phys.* **9** (1941) 341.
4. P. S. THEOCARIS and G. C. PAPANICOLAOU, *Coll. Polym. Sci.* **258** (1980) 1044.
5. M. OCHI, H. LESAKO and M. SHIMBO, *Polymer* **26** (1985) 457.
6. R. E. WETTON, M. R. STONE, and G. E. PRATT, in "Proceedings of conference of the North American Thermal Analysis Society, (NATAS)", San Francisco, Paper 2, (1986).
7. J. CHANG, PhD dissertation, University of Connecticut (1986).
8. J. F. GÉRARD, *Polym. Engng Sci.* **28** (1988), 568.
9. J. CHAUCHARD, B. CHABERT, P. JEANNE and G. NEMOZ, *Angew Makromol. Chem.* **154** (1987) 23.
10. P. PERRET, J. F. GÉRARD and B. CHABERT, *CR Acad. So. Paris* **304** Série II (1987) 569.
11. P. PERRET, J. F. GÉRARD, B. CHABERT, A. DARTUS and J. HOGNAT, "Comptes-Rendus des Sixièmes Journées Nationales sur les Composites, JNC6", Paris, October 1988 (Editions Pluralis, Paris 1988) pp. 103–14.
12. S. IDE, T. TAKAHASHI and A. SHIMAMOTO, in "Controlled Interphases in Composite Materials", edited by H. Ishida (Elsevier Science, London, 1990) pp. 701–06.
13. J. L. THOMASON, *Polym. Compos.* **11** (1990), 105.
14. P. S. CHUA, *ibid.* **8** (1987) 308.
15. *Idem, SAMPE Q.* **18** (1987).
16. J. CINQUIN, B. CHABERT, J. CHAUCHARD, E. MOREL and J. P. TROTIGNON, *Composites* **21** (1990) 141.
17. A. GARTON, J. H. DALLY, W. T. K. STEVENSON and D. M. WILES, *Polym. Engng Sci.* **24** (1986) 2383.
18. C. HUET, Annal. *Ponts Chaussées* **6** (1965) 373.
19. A. T. DiBENEDETTO and P. J. LEX, *Polym. Engng Sci.* **29** (1989) 543.
20. J. G. WILLIAMS, M. E. DONNELLAN, M. R. JAMES and W. L. MORRIS, *Mater. Sci. Engng* **A126** (1990) 305.
21. L. T. DRZAL, M. J. RICH, M. F. KOENIG and P. LLOYD, *J. Adhesion* **16** (1983) 133.
22. J. L. KARDOS, in "Molecular Characterization of Composite Interfaces", edited by H. Ishida and G. Kumar, Polymer Science and Technology Series Vol. 27 (Plenum Press, New York, 1985) pp. 1–11.
23. C. SELLITTI, J. L. KOENIG and H. ISHIDA, *Mater. Sci. Engng* **A126** (1990) 235.
24. M. F. GRENIER-LOUSTALOT and P. GRENIER, *Polymer*, **33** (1992) 1187.
25. G. W. SCHERER, *J. Non-Cryst. Solids* **123** (1990) 75.
26. D. P. ALMOND, O. G. BRADDELL and B. HARRIS, *Polymer* **33** (1992) 2234–2237.
27. M. L. WILLIAMS, R. F. LANDEL and J. D. FERRY, *J. Amer. Chem. Soc.* **77** (1955) 3701.
28. J. SOULETIE and J. L. THOULENCE, *Phys. Rev.* **B32** (1985) 516.
29. P. C. HOHENBERG, and B. I. HALPERIN, *Rev. Mod. Phys.* **49** (1977) 435.
30. A. K. JONSCHER, *Coll. Polym. Sci.* **253** (1975) 231.
31. A. K. JONSCHER, *Nature* **267** (1977) 673.
32. B. Z. JANG, *Compos. Sci. Technol.* **44** (1992) 333.

Received 27 October
and accepted 19 November 1992